# The Discovery of Hydrothermal Vents

# Hydrothermal Plumes in the Galápagos Rift

by

R.F. Weiss, P. Lonsdale, J.E. Lupton,
A.E. Bainbridge, H. Craig

Reprinted from *Nature* Magazine,
Vol. 267, No. 5612: 600-603, June 16, 1977

(Reprinted from Nature, Vol. 267, No. 5612, pp. 600–603, June 16, 1977)


# Hydrothermal plumes in the Galapagos Rift

ALTHOUGH there is indirect evidence that a major fraction of the heat loss from newly-created lithosphere occurs by convection of seawater through the porous crust[1–3], it has proved difficult to locate vents of deep-sea hydrothermal systems by direct measurement of the discharge fluid. Local increases in bottom water temperature up to 0.1 °C have been measured by towing arrays of thermistors a few metres above the axes of active oceanic spreading centres[4,5], but these data are ambiguous because small temperature anomalies may have a hydrographic explanation. We report here the first conclusive measurements of modified seawater discharging as buoyant hydrothermal plumes from fissures in young oceanic crust. We obtained samples of hydrothermal plumes in the Galapagos Rift[3], albeit after considerable dilution with surrounding bottom-water, and report the first results of the collection and analysis of these samples.

Our initial estimates of properties useful for detecting deep-ocean hydrothermal fluids were based on the geochemistry of the Red Sea brines[6,7], the only oceanic geothermal system previously sampled. In this system the basalt-interaction imprint is unfortunately superimposed on a saturated brine because the seawater flows through evaporite deposits before entering the basalts[6]. Predicted concentrations for constituents masked by the evaporite contribution must therefore be based on laboratory measurements[8]. Our estimates showed that helium isotopes were by far the most sensitive geochemical tracers: a mixture of one part of hydrothermal fluid in $\sim 10^5$ parts of seawater should be detectable in the $^3He/^4He$ isotope ratio, while a dilution of $\sim 2 \times 10^4$ should be detectable with total helium concentration. The latter figure is comparable with the detection limit for temperature differences, assuming a 50 °C fluid temperature. Transition metals such as Mn and Fe are also highly enriched in the Red Sea brines but the observed enrichments are consistent with an origin from evaporites[6] and $^3He$ is the only tracer which cannot be derived from such a source[7].

During the May 1976 Pleiades Expedition of the Scripps Institution, near-bottom hydrographic and geochemical surveys of sites on the East Pacific Rise (4°S, 102°W) and in the Galapagos Rift (1°N, 86°W) were made with a remote sensing and sampling system attached to the deep tow geophysical vehicle of the Scripps Marine Physical Laboratory[9]. The geochemical system included a high-precision CTD instrument to measure conductivity, temperature, and pressure, a light transmissometer, and an array of 8 remotely-triggered 9-litre sampling bottles de-

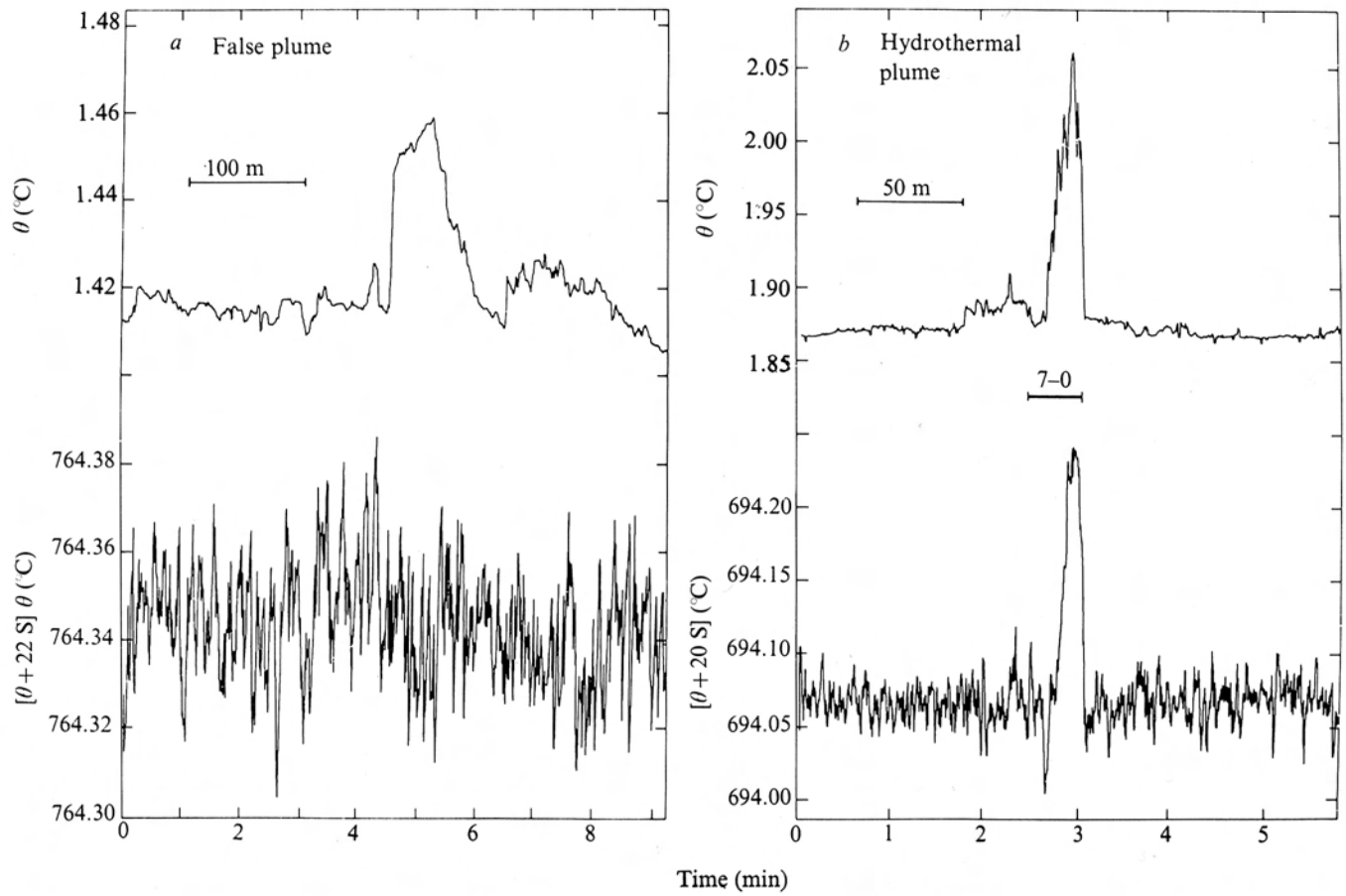


**Fig. 1** Temperature records from an arbitrary time zero as the deep tow vehicle is towed ~ 10 m above bottom. Upper traces: potential temperature (θ) plotted at 10 points $s^{-1}$, corrected for a 200-ms time constant and smoothed by 10-point running average. Lower traces: the θ-salinity function ($\theta + XS$), which is invariant to mixing, with similar correction and smoothing. *a*. A record taken 1.9 km west of the East Pacific Rise axis, shows a 'false plume' in which the temperature spike is not seen in the θ–*S* function and is thus due to mixing. Tow speed was 50 m $min^{-1}$. *b*. The Galapagos Rift site data show a true hydrothermal spike which is reflected in both the temperature and $\theta + XS$ records. Tow speed was 43 m $min^{-1}$ and sample 7–0 was collected during the interval shown beneath the θ record.

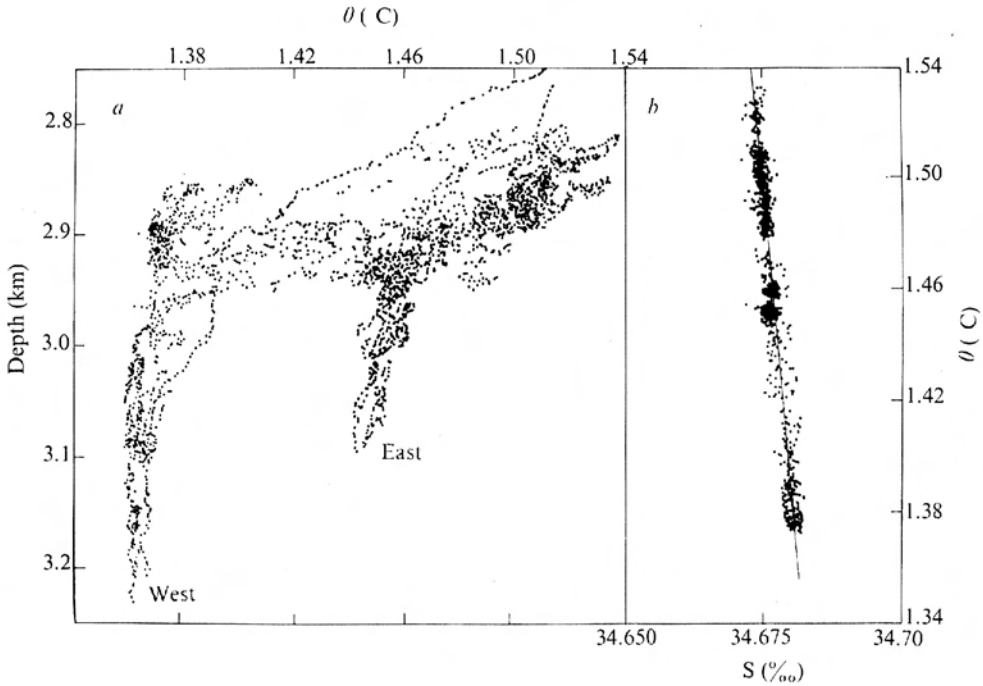


**Fig. 2** Near-bottom (10–100 m) potential temperature data points measured over several hours of towing at the East Pacific Rise survey site, plotted against depth (Fig. 2*a*) and salinity (Fig. 2*b*). The θ–*S* diagram (2*b*) shows that the entire array of water types represents a single water mass; the θ–*S* slope here ($= -X$) is −22.

signed for rapid flushing. The data were telemetered to a shipboard computer which continuously monitored depth, potential temperature ($\theta$), salinity ($S$), potential density at 4,000 decibars ($\sigma_4$), and light transmission in real time. Measurement precision was ±1 m in depth, ±0.0015 °C in $\theta$, and ±0.002‰ in $S$. At each site the instrument package was towed ~8–100 m above bottom at speeds of ~1–2 knots (30–60 m min$^{-1}$) for about four days, using acoustic transponders for navigation and sonars and cameras for mapping bottom topography.

Near-bottom potential temperature excursions or 'spikes' were encountered in both survey areas; two examples are shown in Fig. 1 (upper traces). Hydrographic or mixing spikes ('false plumes') were characterised as such in the following way. The temperature–salinity ($\theta$–$S$) relationship for the local water mass was first established by continuous soundings with the vehicle. The observed $\theta$–$S$ relationship (linear at the spreading axis depth) was then programmed into the computer and the appropriate function of $\theta$,$S$ which is invariant to mixing was monitored continuously. Deviations from this relationship were assumed to represent possible hydrothermal plumes and sampling was triggered manually when such deviations were observed.

Fig. 2 shows $\theta$–$S$ data points collected over several hours of towing during the East Pacific Rise survey. Bottom water temperatures west of the rise in this area are ~0.1 °C lower than at comparable depths east of the rise, while at the crest itself there is a transition region which is actually a sharp benthic thermocline (Fig. 2*a*). Fig. 2*b*, which contains all the rise-crest data from Fig. 2*a*, shows that only a single water mass, characterised by a linear $\theta$–$S$ relationship, is present over the entire region. The transition region at the rise crest thus simply reflects linear mixing between the water types on either side of the crest; as the deep tow vehicle navigates through the rough topography the $\theta$ record exhibits spikes caused by vertical excursions of the sensor and by encounters with various members of the continuous array of water types available in eddies and streams on the crest. Heated bottom water, however, will deviate from the ambient $\theta$–$S$ relationship characterised by $\theta + XS =$ constant, where $X$ is the negative slope on the $\theta$–$S$ plot (Fig. 2*b*). Because of the possibility of conductive heating, the detection of such a '$\theta$–$S$ spike' is a necessary, but not sufficient, condition for the existence of an actual hydrothermal plume.

The lower trace in Fig. 1*a* is the real time record of the $\theta$–$S$ function measured concurrently with the East Pacific Rise $\theta$ record shown above, and plotted to the same vertical scale. This spike is clearly due to mixing and is labelled a 'false plume'. It is apparent that a '$\theta$–$S$ spike' requires an amplitude of >~0.02° for detection due to the scatter introduced by the conductivity measurement. Within this limitation, no hydrothermal spikes were observed during the East Pacific Rise survey.

Fig. 1*b* shows a potential temperature spike measured on the Galapagos Rift which shows a corresponding excursion in the $\theta$–$S$ function. In this area the near-bottom temperature structure reflects mixing between bottom water entering the Panama Basin through the Ecuador Trench[10] and warmer overlying water which spills across the Carnegie Ridge[11]. The $\theta$–$S$ excursion shows clearly that in this case the $\theta$ anomaly is not caused by mixing. Sample 7–0, collected somewhere in the indicated time interval, had a $^3$He/$^4$He ratio equal to twice the atmospheric ratio, a spectacular anomaly relative to 'background' water which has a ratio only 30% greater than atmospheric[12]. This is by far the largest $^3$He/$^4$He ratio yet observed in deep ocean water and there is thus no doubt that an actual hydrothermal plume was sampled.

Fig. 3 shows the bathymetry of the Galapagos Rift area as surveyed during the present study. The lava flows in the inner rift valley are fractured by many small faults and fissures along the rift margins, but near the central axis fracturing is confined to a few fissures about two or three metres wide extending along the central high[13,14]. Ten temperature spikes with corresponding '$\theta$–$S$ spikes' were observed in this region during the shipboard survey; the locations of these ten spikes are plotted in Fig. 3 which shows that all ten lie on the axial fissure in the centre of the inner rift. Three of these spikes, 7–0 (the largest of the ten spikes) 8–3, and 8–6, were sampled and analysed; all three showed $^3$He/$^4$He and radon anomalies relative to background water, verifying that the $\theta$–$S$ excursions in these ten locations represent true hydrothermal plumes.

A preliminary analysis of the remaining tow data has shown no evidence of hydrothermal activity off the central

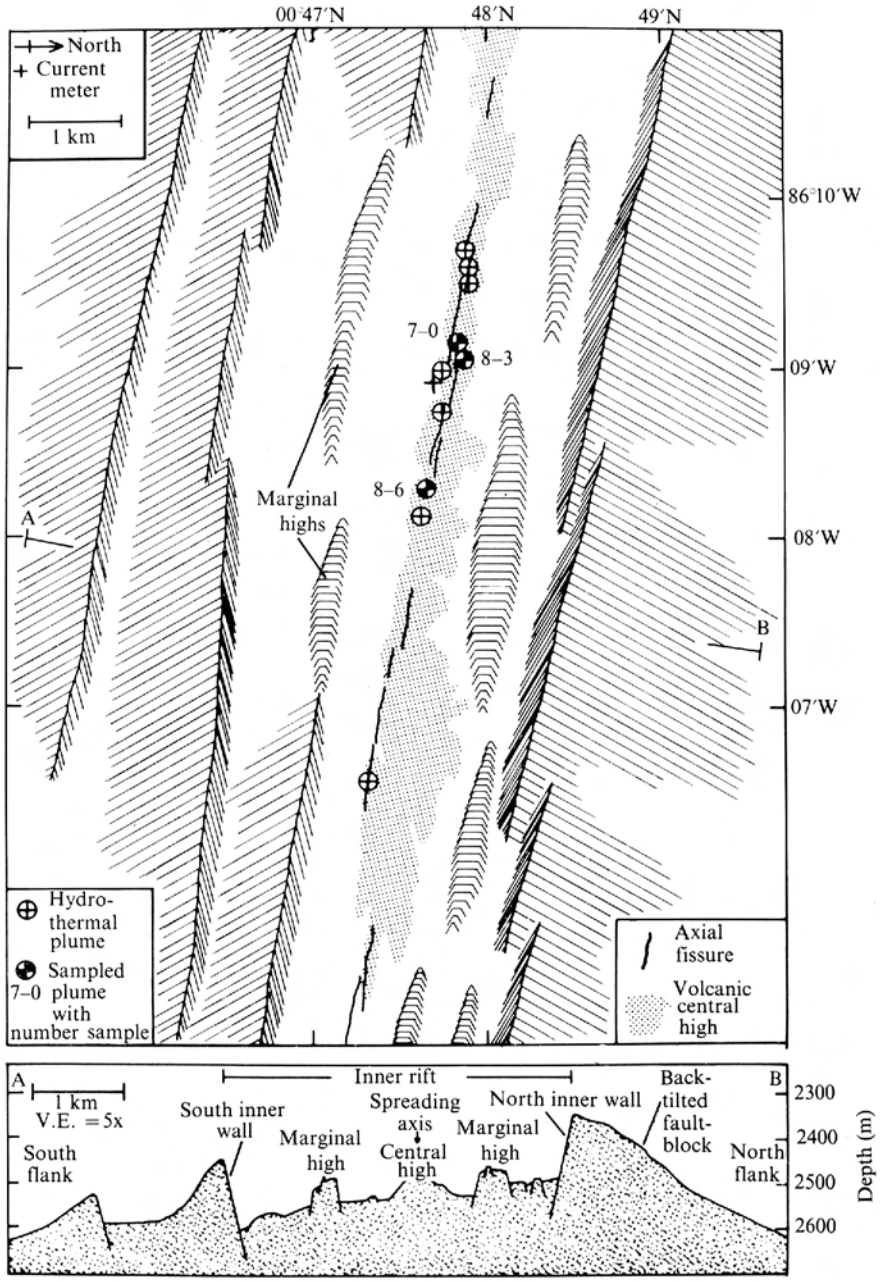


**Fig. 3** Locations of hydrothermal plumes observed in the Galapagos Rift, with topography summarised from a deep tow structural map[14]. Numbers refer to plumes actually sampled. In addition to the axial fissures shown there are many fissures and minor faults along the minor rift margins; no plumes were detected in these marginal areas.

axis of the Galapagos Rift. One area of special interest in our survey was a region of 5–20 m high sediment mounds ~30 km south of the central axis which have been described as possible hydrothermal vents[13]. In this area the water structure is so uniform that hydrothermal spikes of ~0.002 °C should be observable, yet even with this sensitivity there was no evidence of hydrothermal plumes associated with the mounds.

Several of the hydrothermal plumes showed a small decrease (~0.1%) in light transmission; filtrates from the three sampled plumes and water have been distributed for a number of geochemical measurements. The helium and radon measurements are described in an accompanying paper[12]. Our results show that there is a one-to-one correspondence between the hydrographic identification of samples as heated water and the presence of excess quantities of $^3He/^4He$ and Rn in these samples. Together, these results constitute the first conclusive identification and sampling of hydrothermally circulating seawater in a deep-ocean spreading centre. Based on these findings, a detailed study of the Galapagos Rift hydrothermal vents using a manned submersible is now in progress.

We thank F. N. Spiess, J. Spiegelberg, J. Jain, and the entire Deep Tow technical group for their support, interest and assistance. Financial support for this research was provided by the US NSF.

R. F. Weiss
P. Lonsdale
J. E. Lupton
A. E. Bainbridge
H. Craig

*Scripps Institution of Oceanography, University of California, San Diego La Jolla, California 92093*

Received 21 March; accepted 14 April 1977.

1 Talwani, M., Windisch, C. C. & Langseth, M. G. *J. Geophys. Res.* **76**, 473–517 (1971).
2 Lister, C. R. B. *Geophys. J.R. astr. Soc.* **26**, 515–535 (1972).
3 Sclater, J. G. & Klitgord, K. D. *J. Geophys. Res.* **78**, 6951–6975 (1973).
4 Williams, D. L., Von Herzen, R. P., Sclater, J. G. & Anderson, R. N. *Geophys, J.R. astr. Soc.* **38**, 587–608 (1974).
5 Rona, P. A., McGregor, B. A., Betzer, P. R. & Krause, D. C. *Deep-Sea Res.* **22**, 611–618 (1975).

(Reprinted from Nature, Vol. 267, No. 5612, pp. 603–604, June 16, 1977)


# Mantle helium in hydrothermal plumes in the Galapagos Rift

THE $^3He/^4He$ ratio in deep Pacific water is 20–30% higher than in atmospheric helium because of injection of primordial helium from the mantle[1,2]. The largest $^3He$ enrichments in the Pacific have been found in water on the crest of the East Pacific Rise where the isotopic ratios indicate[2] that the excess helium component has a $^3He/^4He$ ratio about ten times the atmospheric ratio, in agreement with the ratios measured in trapped helium in the glassy rims of oceanic tholeiites[3,4]. Recent measurements in this laboratory[5] have shown that the hot brines in the axial rift of the Red Sea are very highly enriched in mantle helium. $^3He$ and $^4He$ are respectively 3300 and 380 times supersaturated relative to atmospheric solubility equilibrium in seawater, with a $^3He/^4He$ ratio of $1.2\times10^{-5}$, or 8.6 times the ratio in atmospheric helium. Comparison of the enrichments of various elements in the Red Sea brines and in brines associated with salt domes[6] shows that helium is the only component in the Red Sea brines which unequivocally requires derivation from hydrothermal circulation of seawater in basalts. The helium isotopes are thus an extremely powerful and sensitive tracer for the detection and mapping of hydrothermal systems in oceanic spreading centres.

The Red Sea brines represent an extreme example of the most probable mechanism for the actual injection of mantle helium into the deep sea, namely the penetration and hydrothermal circulation of seawater in basalts on the crests of mid-ocean rises. In the Red Sea the circulating fluid is a brine because the downward penetrating seawater encounters evaporites before reaching the basalt[6], and thus the upward convecting fluid is stabilised in brine pools in depressions on the sea floor. In normal oceanic spreading centres, however, where evaporites are absent, the heated seawater should emerge as hydrothermal plumes which should be detectable by the association of temperature anomalies with the mantle helium signature. In this letter we report the first $He^3$ measurements on such plume samples, showing that hydrothermal circulation of seawater in basalts is an active process at spreading centres which transfers mantle helium to deep ocean water.

In May 1976 nine samples of bottom water were collected along the central axis of the Galapagos Spreading Center[7,8] using a newly-devised hydrographic sampling sled[9,10] attached to the Scripps Institution of Oceanography deep-tow instrument. The location of the samples relative to the local topography is described in the accompanying paper[10]. Three of these samples were collected during 'hydrothermal spike' temperature excursions whose origin could not be explained by turbulent mixing within the ambient water mass. The samples were taken about 10 m above the axial fissure opening, at the same level as the CTD sensor which recorded the temperature anomalies. When the sled was recovered, samples for helium analysis were sealed in copper tubing pinch-clamp containers and returned to the laboratory for analysis on a $^3He/^4He$ ratio mass spectrometer as described previously[3,5]. Radon activities were measured at sea on six of these samples, using our normal shipboard extraction and counting techniques[11] with the exception that the analyses were made on one, rather than twenty, litres of water.

Table 1 lists the $^3He$ results on the three samples taken during temperature spikes (7–0, 8–3, and 8–6) and on the samples of normal or 'background' bottom water where no temperature anomalies were observed on the continuous tow record. The measurements are tabulated as percent deviations of the $^3He/^4He$ ratio ($R$) from the atmospheric ratio ($1.40\times10^{-6}$), that is

$$\delta(^3He) = 100\,[(R/R_{Atm})-1)]$$

The mean background water anomaly is $\delta(^3He) = 30.4\%$, in excellent agreement with values of 30.3 and 31.0% observed on the crest and at the mid-depth $^3He$ maximum on the eastern flank of the East Pacific Rise, south and west of the present area[2]. Relative to this background water, which is presumably the water entering the hydrothermal system, the $^3He/^4He$ ratio in sample 7–0 is enriched by 53% (1.99/1.30). The other two plume samples are also enriched in $^3He$ relative to ambient background, but by much smaller amounts. The $\delta(^3He)$ value of 99% measured on sample 7–0 is by far the largest value yet observed in ocean waters, and establishes for the first time a clear connection between the mantle helium in oceanic basalts and the excess $^3He$ observed in the deep oceans, by seawater penetration and circulation in the basalts.

Radon concentrations (Table 1) are reported as 'excess radon' relative to the activity of $^{226}Ra$. The $^{226}Ra$ activity was assumed to be 33 d.p.m. per 100 kg from a previous study by this laboratory[11] on bottom waters 29 km south-west of the present location in approximately the same depth; rough measurements made on the present small samples were in agreement within the larger errors. The excess radon concentrations in the three plume samples (80–229 d.p.m. per 100 kg) are clearly much greater than the background value of about forty, although they do not scale with the $^3He$ anomalies. Because of the short radioactive mean life (5.5 d) the $^{222}Rn$ enrichments in plume waters are probably due to extraction of radon from the basalts, although some contribution from sediment material trapped within the axial fissure cannot be excluded.

Fig. 1 shows the absolute $^3He$ and $^4He$ concentrations in the deep tow samples, together with atmospheric solubility values and vectors for addition of atmospheric helium to air-saturated deep water, and for addition of radiogenic $^4He$ and pure 'mantle helium' (basalt values[3,4]) to background water

**Table 1** $^3He$ and $^{222}Rn$ measurements on hydrothermal plume and background water on the Galapagos Rift (~0°48′N, 85°55′W)

| Tow no., bottle no. | $\delta(^3He)$ (%) | Excess $^{222}Rn$ (d.p.m. per 100 kg) |
|---|---|---|
| *a* Samples with potential–temperature spikes | | |
| 7–0* | 99.3 | 191 |
| 8–3 | 35.7 | 80 |
| 8–6 | 42.6 | 229 |
| *b* 'Background water' | | |
| 7–1 | 27.8 | 39 |
| 7–2 | — | 49 |
| 8–1 | 28.6 | — |
| 8–2 | 30.2 | 33 |
| 8–5 | 33.4 | — |
| 8–7 | 32.2 | — |
| Mean | 30.4±2 | 40±8 |

Radon precision = ±3 d.p.m. per 100 kg (counting error); $^{226}Ra$ activity assumed = 33 d.p.m. per 100 kg. $^3He/^4He$ ratios are accurate to ±0.7% in $\delta(^3He)$.

*The temperature spike for sample 7–0 is shown in Fig. 1 of ref. 10; samples 8–3 and 8–6 were collected from plumes showing smaller temperature spikes.

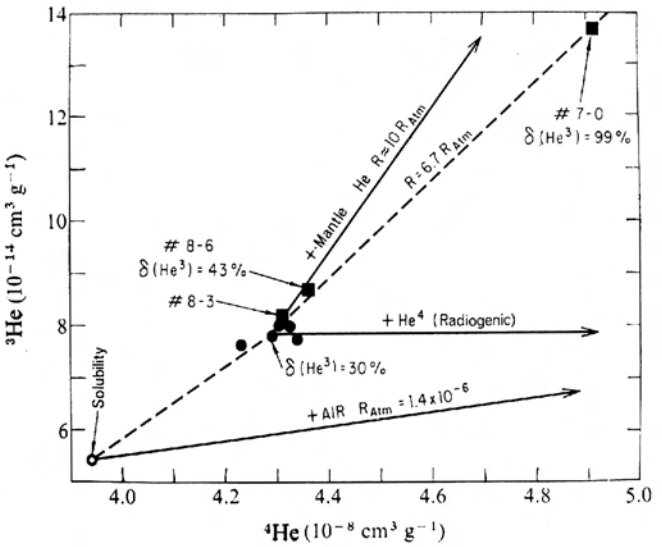


**Fig. 1** $^3$He and $^4$He concentrations in water samples with temperature spikes (squares) and in ambient 'background water' (circles) on the axial fissure of the Galapagos Rift. The point labelled 'solubility' indicates the equilibrium air saturation concentrations for deep water. ● Normal bottom waters; ■ Hydrothermal plumes.

on the Galapagos spreading centre. (The 'absolute' concentrations, based on preliminary 'peak-height' determinations for $^4$He, are accurate to about 5%; more accurate isotope dilution measurements are in progress.) $^3$He and $^4$He enrichments in the ambient background water relative to equilibrium solubility represent the net effect of air injection[12] and addition of mantle and radiogenic helium to deep water during its circulation. The absolute helium anomalies in sample 7–0 are very much larger: $^3$He and $^4$He concentrations are respectively 75% and 14% greater in this sample than in the mean Galapagos background water.

The added increment of $^3$He relative to background water is $5.9\times10^{-14}$ cm$^3$ STP per g in sample 7–0, an amount approximately equal to the initial solubility equilibrium (Fig. 1) and thus about 0.03% of the $^3$He concentration observed in the Red Sea brines. The estimated temperature of inflowing Red Sea brines is ~100 °C (ref. 13); thus if the hydrothermal systems in Red Sea and Galapagos basalts are at all similar, a temperature spike of ~0.03 °C is predicted for sample 7–0, in reasonable agreement with the signal observed during sampling[10].

In Fig. 1 the vector from the mean background water to sample 7–0 corresponds to addition of helium with $^3$He/$^4$He = $9.4\times10^{-6}$ or $R = 6.7R_{Atm}$, significantly lower than the 'mantle helium' ratio ($R \sim 10R_{Atm}$) observed in ocean-ridge basalts[3,4], which implies that about 30% of the added helium is radiogenic $^4$He generated in the oceanic crust. Helium with $R = 6.7\ R_{Atm}$ would be found in Pacific ridge-basalts after about 30 my of $^4$He production (ref. 4), an age far too great for basalts in such close proximity to the rift axis. The holocrystalline portions of pillow basalts exchange trapped gases with seawater on a much shorter time scale than this[14]; thus the helium isotope ratios in basalt-seawater hydrothermal systems probably decrease coutinuously with time as the initial mantle helium component is progressively stripped out by the fluid phase and the radiogenic component grows in. It may therefore be possible to characterise such hydrothermal systems in time and space by detailed mapping of helium isotope ratios in plume samples.

The extreme sensitivity of helium and radon for plume detection is indicated by our estimate that sample 7–0 contained of the order of 0.03% of hydrothermal water. A sample with a 1 °C temperature spike would, on this basis, contain helium with $R \sim 5.5R_{Atm}$ and a $^{222}$Rn activity of ~ 5,000 d.p.m. per 100 kg. Radon is of course a radiogenic isotope which is present in very high activity in marine sediments; it is therefore not a completely unamiguous tracer for seawater which has penetrated basalts. The $^3$He signature, however, provided unequivocal evidence for the existence of a hydrothermal basalt–seawater system in the axial region of the Galapagos Rift.

We thank Dr F. N. Spiess for his strong interest and encouragement in this work, P. Lonsdale for discussion and for assistance at sea, A. Birket for assistance in the laboratory, and the Ocean Sciences section of the US NSF for financial support.

J. E. Lupton
R. F. Weiss
H. Craig

*Isotope Laboratory,*
*Scripps Institution of Oceanography,*
*University of California, San Diego,*
*La Jolla, California 92093*

Received 21 March; accepted 14 April 1977.

1 Clarke, W. B., Beg, M. A. & Craig, H. *Earth planet. Sci. Lett.* **6**, 213 (1969).
2 Craig, H., Clarke, W. B. & Beg, M. A. *Earth planet. Sci. Lett.* **26**, 125 (1975).
3 Lupton, J. E. & Craig, H. *Earth planet. Sci. Lett.* **26**, 133 (1975).
4 Craig, H. & Lupton, J. E. *Earth planet. Sci. Lett.* **31**, 369 (1976).
5 Lupton, J. E., Weiss, R. F. & Craig, H. *Nature* **266**, 244 (1977).
6 Craig, H., *Hot Brines and Recent Heavy Metal Deposits in the Red Sea*, (eds Degens, E. T. and Ross, D. A.) 208–242 (Springer-Verlag, New York, 1969).
7 Sclater, J. G. & Klitgord, K. D. *J. geophys. Res.* **78**, 6951 (1973).
8 Williams, D. L., Von Herzen, R. P., Sclater, J. G. & Anderson, R. N. *Geophys. J. R. Astr. Soc.* **38**, 587 (1974).
9 Weiss, R. F. *et al.*, *Trans. Am. Geophys. Union* **57**, 935 (1976).
10 Weiss, R. F. *et al. Nature* **267**, 600–603 (1977).
11 Chung, Y–C & Craig, H. *Earth planet. Sci. Lett.* **14**, 55 (1972).
12 Craig, H. & Weiss, R. F. *Earth planet. Sci. Lett.* **10**, 289 (1971).
13 Ross, D. A. *Science* **175**, 1455 (1972).
14 Dymond, J. & Hogan, L. *Earth planet. Sci. Lett.* **20**, 131 (1973).

Printed in Great Britain by Henry Ling Ltd., at the Dorset Press, Dorchester, Dorset

6 Craig, H. *Hot Brines and Recent Heavy Metal Deposits in the Red Sea* (eds Degens, E. T. & Ross, D. A.) Springer-Verlag, New York, 208–242 (1969).
7 Lupton, J. E., Weiss, R. F. & Craig, H. *Nature* **266**, 244–246 (1977).
8 Bischoff, J. L. & Dickson, F. W. *Earth Planet. Sci. Lett.* **25**, 385–397 (1975).
9 Spiess, F. N. & Mudie, J. D. *The Sea* (ed. Maxwell, A. E.) 205–220 (John Wiley and Sons, New York, 1970).
10 Laird, N. P. *J. Mar. Res.* **29**, 226–234 (1971).
11 Detrick, R. S., Williams, D. L., Mudie, J. D. & Sclater, J. G. *Geophys. J.R. astr. Soc.* **38**, 627–637 (1974).
12 Lupton, J. E., Weiss, R. F. & Craig, H. *Nature* **267**, 603–605 (1977).
13 Klitgord, K. D. & Mudie, J. D. *Geophys. J.R. astr. Soc.* **38**, 563–586 (1974).
14 Lonsdale, P. *Geology* **5**, 147–152 (1977).

Printed in Great Britain by Henry Ling Ltd., at the Dorset Press, Dorchester, Dorset